To appear in the *Astrophysical Journal Letters.*

Accretion Rates onto Massive Black Holes in Four Quiescent Elliptical Galaxies

J. M. Wrobel and J. R. Herrnstein[1]

National Radio Astronomy Observatory, P.O. Box O, Socorro, New Mexico 87801

jwrobel@nrao.edu, jherrnst@nrao.edu

ABSTRACT

Four quiescent elliptical galaxies were imaged with the NRAO VLA at 8.5 GHz. Within the context of canonical advection-dominated accretion flows (ADAFs), these VLA images plus published black hole masses constrain the accretion rates to be $< 1.6 \times 10^{-4}$, $< 3.6 \times 10^{-4}$, $\leq 7.8 \times 10^{-4}$, and $\leq 7.4 \times 10^{-4}$ of the Eddington rates. These ADAF accretion rates derived at 8.5 GHz have important implications for the levels of soft and hard X-rays expected from these quiescent galaxies.

Subject headings: accretion, accretion disks - galaxies: individual (NGC 4291, NGC 4564, NGC 4621, NGC 4660) - galaxies: nuclei - radio continuum: galaxies - X-rays: galaxies

1. MOTIVATION

Evidence is accumulating that nearby galactic nuclei commonly harbour massive dark objects (Magorrian et al. 1998). These objects are probably black holes, because such remnants from the QSO era should be common (Fabian & Rees 1995) and because some nuclear star clusters with the requisite mass and size would be improbably younger that their host galaxies (Maoz 1998). Given a black hole mass, $M_{\rm BH}$, a next important step is to constrain the rate, $\dot{M}$, at which material is being accreted onto the black hole. Associated with any black hole is its Eddington accretion rate, $\dot{M}_{\rm E}$, which is the rate necessary to sustain the Eddington luminosity. For a 10% radiative efficiency and $M_{\rm BH} = 10^8 m_8\ M_\odot$, $\dot{M}_{\rm E} = 2.2 m_8\ M_\odot\ {\rm yr}^{-1}$. For giant elliptical galaxies hosting black holes, accretion-rate estimates have long been available for comparison with Eddington rates (Fabian & Canizares 1988; Mahadevan 1997). These estimates are based on Bondi (1952) accretion from an interstellar medium with temperature $T = 10^7 T_7$ K and pressure $P = 10^6 P_6$ cm^{-3} K, with the accretion being characterized by a Bondi radius $r_{\rm B} \sim 4.3 m_8 T_7$ pc and a Bondi rate

[1]Current address: Renaissance Technologies Corporation, 600 Route 25A, East Setauket, NY 11733-1249

$\dot{M}_{\rm B} \sim 1.9 \times 10^{-4} m_8 P_6 T_7 \ M_\odot \ {\rm yr}^{-1}$. Then a black hole with $m_8 = 1$ in a medium with $P_6 = 1$ and $T_7 = 1$ will accrete at a Bondi rate $\dot{M}_{\rm B} \sim 1.9 \times 10^{-4} \ M_\odot \ {\rm yr}^{-1}$, which is almost four orders of magnitude less than the associated Eddington rate of $\dot{M}_{\rm E} = 2.2 \ M_\odot \ {\rm yr}^{-1}$. The Bondi rate estimates are therefore extremely sub-Eddington. Still, such low rates could be pervasive among nearby ellipticals and, moreover, could define a minimum level of activity for ellipticals hosting massive black holes

This Letter examines the consequences, in the radio and X-ray regimes, of such low accretion rates in nearby elliptical galaxies. The approach is to obtain deep radio continuum images of four ellipticals studied by Magorrian et al. (1998) and then interpret those images within the context of canonical advection-dominated accretion flows (ADAFs), reviewed recently by Narayan, Mahadevan, & Quataert (1998). The radio continuum from an ADAF is thermal synchrotron emission from a magnetized plasma, and the conversion between the ADAF radio power, P_ν, and the ADAF accretion rate, $\dot{M}_{\rm A}$, is relatively straightforward if the black hole mass is known (Mahadevan 1997; Yi & Boughn 1998). Recent efforts along these lines have focused on galaxies with significant radio emission from nonthermal synchrotron jets (Di Matteo et al. 2000). In constrast, this study examines four quiescent elliptical galaxies previously undetected at radio wavelengths (Wrobel 1991; Wrobel & Heeschen 1991), thereby minimizing one of the largest potential complications in an ADAF analysis - the role of jet outflows. Further evidence for the quiesence of these four galaxies comes from their use as absorption-line templates in optical spectroscopic studies (Ho, Filippenko, & Sargent 1997), plus their weak or undetected X-ray emission (Beuing et al. 1999). For these four quiescent ellipticals, the new radio imaging constrains the ADAF accretion rates to be $< 1.6 \times 10^{-4}$, $< 3.6 \times 10^{-4}$, $\leq 7.8 \times 10^{-4}$, and $\leq 7.4 \times 10^{-4}$ of the Eddington rates. These ADAF accretion rates derived at 8.5 GHz have important implications for the levels of X-ray emission expected from these quiescent galaxies.

2. OBSERVATIONS AND IMAGING

The Very Large Array (VLA), described by Thompson et al. (1980), was used 1999 May 6-7 UT in its 1-km configuration to observe NGC 4291, NGC 4564, NGC 4621, and NGC 4660. Data were acquired in dual circular polarizations and at a center frequency 8.4601 GHz with bandwidth 100 MHz. Observations were made assuming a coordinate equinox of 2000. The phase calibrator J1153+8058 was used for NGC 4291, while J1239+0730 was used for the other three galaxies. Scheduled on-source integration times were 105-120 minutes. The galaxies were observed at *a priori* positions from the Digitized Sky Survey (DSS) web site. Improved DSS positions with 1-D error estimates, $\sigma_{\rm DSS}$, have since become available (Cotton, Condon, & Arbizzani 1999) and will be used below. $\sigma_{\rm DSS}$ depends in part on the galaxy major axis, $\theta_{\rm M}$, and values for both terms appear in Table 1. Observations of 3C 286 were used to set the amplitude scale to an accuracy of about 3%. The data were calibrated using the 1999 October 15 release of the NRAO AIPS software. No self-calibrations were performed.

The AIPS task IMAGR was used to form and deconvolve images of the Stokes IQU emission from each galaxy. All images were made with natural weighting to optimize sensitivity. The Stokes I images appear in Figure 1, with crosses indicating the the DSS positions and their errors. The large ellipses shown in three panels outline the galaxies' major and minor diameters and elongation position angles (Wrobel 1991). The corresponding ellipse for NGC 4621 falls beyond the panel boundaries. For each panel the table gives the image resolution, $R_{8.5\mathrm{GHz}}$, expressed as the FWHM dimensions and elongation orientation of the elliptical-Gaussian restoring beam; the image rms value, $\sigma_{8.5\mathrm{GHz}}$, in units of microjanskys per beam area (μJy ba^{-1}); and the image scale, s, based on the distance, D, from Magorrian et al. (1998) for $\mathrm{H}_0 = 80$ km s^{-1} Mpc^{-1}. Each galaxy image was searched for an emission peak $S_{8.5\mathrm{GHz}} > 4\sigma_{8.5\mathrm{GHz}}$ within a circular region of radius 4 σ_{DSS}. The resulting peak strengths appear in the table. For the two detected galaxies, quadratic fits in the image plane yielded the peak flux densities tabulated, along with their errors that are quadratic sums of a 3% scale error and $\sigma_{8.5\mathrm{GHz}}$. Those fits also yielded the following radio positions, along with their 1-D errors, σ_{VLA}, which are dominated by the peak signal-to-noise ratio (Ball 1975): for NGC 4621, $\alpha(J2000) = 12^h42^m02^s.50$, $\delta(J2000) = 11°38'48''.6$, and $\sigma_{\mathrm{VLA}} = 0''.4$; for NGC 4660, $\alpha(J2000) = 12^h44^m32^s.35$, $\delta(J2000) = 11°11'26''.6$, and $\sigma_{\mathrm{VLA}} = 0''.7$. Each detected galaxy is less than 40% linearly polarized.

3. IMPLICATIONS

Radio continuum can be due to thermal synchrotron emission from an ADAF onto a black hole, nonthermal synchrotron jets emerging from an ADAF, or nonthermal synchrotron jets emerging from a standard accretion disk which itself emits no radio photons. In the radio regime, this Letter analyzes only thermal synchrotron emission from an ADAF. The distances, D, from Magorrian et al. (1998) are used to convert the new 8.5-GHz detections or limits to the observed powers, $P_{8.5\mathrm{GHz}}$, given in the table. These rank among the the most sensitive radio powers, or power limits, available in the literature for elliptical galaxies (Wrobel & Heeschen 1991). Because emission from nonthermal synchrotron jets could account for some unknown fraction of the radio detections, the observed peak flux densities will in general impose upper limits to any ADAF powers, $P_{8.5\mathrm{GHz}}$.

The radio power, P_ν, predicted for an ADAF at a frequency, ν, depends upon: α, the standard Shakura-Sunyaev parametrization of the kinematic viscosity in the accretion flow; β, the ratio of gas pressure to total pressure; m_8, the black hole mass in units of 10^8 $M_\odot$; $\dot{m}_{\mathrm{A}}$, the ADAF accretion rate normalized to the Eddington rate; and T_e, the equilibrium temperature of the electrons (Mahadevan 1997; Yi & Boughn 1998). Canonical ADAFs adopt $\alpha = 0.3$ and an equipartition $\beta = 0.5$. Moreover, for most cases of interest T_e is fairly insensitive to the other model parameters, so an intermediate value of 2.5×10^9 K is adopted. These values for α, β, and T_e then predict that, at frequency $\nu = 8.5$ GHz,

$$P_{8.5\mathrm{GHz}} = 6.7 \times 10^{21} m_8^{\frac{6}{5}} \dot{m}_{\mathrm{A}}^{\frac{6}{5}} \text{ W Hz}^{-1}. \quad (1)$$

The values for $P_{8.5\mathrm{GHz}}$ from this work and for m_8 from Magorrian et al. (1998), when inserted into Equation (1), result in the normalized ADAF accretion rates, $\dot{m}_{\mathrm{A}}$, given in the table. These normalized ADAF rates are highly sub-Eddington, being $< 1.6 \times 10^{-4}$, $< 3.6 \times 10^{-4}$, $\leq 7.8 \times 10^{-4}$, and $\leq 7.4 \times 10^{-4}$ of the Eddington rates. The latter two cases correspond to the galaxies with radio continuum detections. Canonical ADAFs exisit only at normalized accretion rates below a critical rate, $\dot{m}_{\mathrm{crit}} \sim 0.3\alpha^2 = 0.027$ (Esin, McClintock, & Narayan 1997). The normalized rates, $\dot{m}_{\mathrm{A}}$, in the table easily meet this consistency check for canonical, and other reasonable, values of α. For the four quiescent ellipticals in this study, the black hole masses from Magorrian et al. (1998) yield the tabulated Eddington accretion rates, $\dot{M}_{\mathrm{E}}$. Those rates are used to convert the normalized ADAF rates, $\dot{m}_{\mathrm{A}}$, in the table into the absolute ADAF rates, $\dot{M}_{\mathrm{A}}$, also entered in the table.

The ADAF accretion rates derived at 8.5 GHz, in both normalized ($\dot{m}_{\mathrm{A}}$) and absolute ($\dot{M}_{\mathrm{A}}$) form, have consequences for the predicted levels of X-ray emission from these quiescent elliptical galaxies, and these predicted levels must not violate the observed levels. Only one galaxy, NGC 4291, is a weak X-ray emitter and the other three remain undetected in the ROSAT All Sky Survey (Beuing et al. 1999). That survey was conducted with the Position Sensitive Proportional Counter at soft X-rays (0.5-2 keV) and at an angular resolution of $\sim 0.5'$. The table gives values for, or upper limits to, the observed soft X-ray luminosities, L_{RASS}, scaled to the Magorrian et al. (1998) distances. No deprojection analysis has yet been attempted for NGC 4291, since no ROSAT data from the High Resolution Imager are available. Data at hard X-rays (2-10 keV) are also lacking.

An elliptical galaxy harboring an ADAF will be a source of X-rays from the ADAF itself and from the galaxy's interstellar medium. Each photon source will be discussed in turn. The normalized ADAF accretion rates derived at 8.5 GHz are so low that bremsstrahlung emission, not inverse Compton scattering, will dominate the ADAF's X-rays (Mahadevan 1997; Yi & Boughn 1998). The latter authors provide an expression for the bremsstrahlung luminosity of a canonical ADAF that, at the T_e adopted for Equation (1), reduces to

$$L_{\mathrm{A,1keV}} = 1.2 \times 10^{45} m_8 \dot{m}_{\mathrm{A}}^2 \text{ erg s}^{-1} \tag{2}$$

at a fiducial soft X-ray frequency of $\nu = 2.42 \times 10^{17}$ Hz; and reduces to

$$L_{\mathrm{A,6keV}} = 7.2 \times 10^{45} m_8 \dot{m}_{\mathrm{A}}^2 \text{ erg s}^{-1} \tag{3}$$

at a fiducial hard X-ray frequency of $\nu = 1.45 \times 10^{18}$ Hz. Applying the tabulated values for m_8 and $\dot{m}_{\mathrm{A}}$ to Equations (2) and (3) yields the tabulated predictions for the soft and hard X-ray luminosities of the ADAFs. The predicted luminosities at 1 keV are consistent with the published ROSAT limits for NGC 4564, NGC 4621, and NGC 4660, as well as for the ROSAT detection of NGC 4291 but only if that detection is dominated by the galaxy's interstellar medium rather than by its ADAF (Beuing et al. 1999). Note further that the ADAFs are expected to be six times more luminous at hard than at soft X-rays, so these galaxies must must be considered prime targets for observations in the 2-10 keV region with the Advanced Satellite for Cosmology and Astrophysics (Tanaka, Inoue, & Holt 1994).

Soft X-rays can also arise from an elliptical's general interstellar medium (Fabian & Canizares 1988; Mahadevan 1997; Di Matteo et al. 2000). For the galaxies in this study, a Bondi analysis of that medium can produce an estimate for the Bondi accretion rate, $\dot{M}_{\rm B}$, which can then be compared with the absolute ADAF accretion rate, $\dot{M}_{\rm A}$, derived at 8.5 GHz. The black hole masses from Magorrian et al. (1998), in combination with $T_7 = 1$ being typical for elliptical galaxies (Di Matteo et al. 2000), results in the Bondi radii listed in the table. Assuming further that the pressure, $P = 10^6 P_6$ cm^{-3} K, at the Bondi radius satisfies $P_6 = 1 - 10$ (Di Matteo et al. 2000), then the table gives the corresponding range in Bondi accretion rates, $\dot{M}_{\rm B}$. The Bondi rate estimates for $P_6 = 1$ are generally consistent with the limits on the absolute ADAF rates, $\dot{M}_{\rm A}$, imposed at 8.5 GHz, although there is an order-of-magnitude discrepancy in the case of NGC 4291. In constrast, for $P_6 = 10$ the Bondi rates exceed the ADAF rates for all four galaxies. Meaningful comparions between $\dot{M}_{\rm B}$ and $\dot{M}_{\rm A}$ must clearly await a reliable pressure profile for ellipticals in general or, better still, for the galaxies in this study. Futhermore, integration over any adopted pressure profile should not violate $L_{\rm RASS}$ listed in the table.

Further radio observations to quantify any jet contamination in NGC 4621 and NGC 4660 are also needed, for two reasons. First, removal of jet contamination leads to reduced ADAF emission, which in turn implies even lower ADAF accretion rates. Second, the presence of jet emission could signify the importance of physical processes ignored in canonical ADAF models and explored by Di Matteo et al. (2000). Follow-up VLA imaging at other frequencies, ν, but at matched angular resolutions would help assess jet contamination: the flux density from an ADAF-dominated source is expected to rise as $\nu^{\frac{1}{3}-\frac{2}{5}}$ (Mahadevan 1997; Yi & Boughn 1998), whereas the flux density from a jet-dominated source is expected to exhibit a flatter spectral slope. Although the 500-μJy ba^{-1} upper limits at 5 GHz from Wrobel & Heeschen (1991) do have similar resolutions, they are too insensitive to impose useful constraints on spectral slopes between 5 and 8.5 GHz. Moreover, higher-resolution imaging with the NRAO VLBA could provide morphological evidence for nonthermal synchrotron jets and spatially separate jet from ADAF emission, as was successfully done for the spiral galaxy NGC 4258 (Herrnstein et al. 1998). Finally, the image rms values, $\sigma_{8.5{\rm GHz}}$, achieved in this study required 2 hours of integration time. Similar values for $\sigma_{8.5{\rm GHz}}$ will be achieved after a 2-minute integration with the expanded VLA (NRAO 2000). This will make it feasible, for the first time, to target all radio-quiescent ellipticals studied by Magorrian et al. (1998), which should significantly advance our understanding of advection-dominated accretion flows as a new class of extragalactic radio emitters.

The authors thank Dr. R. Mahadevan for discussions. This research has made use of the NASA/IPAC Extragalactic Database (NED) which is operated by the Jet Propulsion Laboratory, Caltech, under contract with the National Aeronautics and Space Administration. The Digitized Sky Surveys were produced at the Space Telescope Science Institute under U.S. Government grant NAG W-2166. The National Geographic Society - Palomar Observatory Sky Atlas (POSS-I) was made by the California Institute of Technology with grants from the National Geographic Society. The Second Palomar Observatory Sky Survey (POSS-II) was made by the California Institute of

Technology with funds from the National Science Foundation, the National Geographic Society, the Sloan Foundation, the Samuel Oschin Foundation, and the Eastman Kodak Corporation. NRAO is a facility of the National Science Foundation operated under cooperative agreement by Associated Universities, Inc.

REFERENCES

Ball, J. A. 1975, in Methods in Computational Physics, Volume 14, eds. B. Alder, S. Fernbach, & M. Rotenberg (New York: Academic Press), 177

Beuing, J, Dobereiner, S., Bohringer, H., & Bender, R. 1999, MNRAS, 302, 209

Bondi, H. 1952, MNRAS, 112, 195

Cotton, W. D., Condon, J. J., & Arbizzani, E. 1999, ApJS, 125, 409

Di Matteo, T., Quataert, E., Allen, S. W., Narayan, R., & Fabian, A. C. 2000, MNRAS, 311, 507

Esin, A. A., McClintock, J. E., & Narayan, R. 1997, ApJ, 489, 865

Fabian, A. C., & Canizares, C. R. 1988, Nature, 333, 829

Fabian, A. C., & Rees, M. J. 1995, MNRAS, 277, L55

Herrnstein, J. R., Greenhill, L. J., Moran, J. M., Diamond, P. J., Inoue, M., Nakai, N., & Miyoshi, M. 1998, ApJ, 497, L69

Ho, L. C., Filippenko, A. V., & Sargent, W. L. W. 1997, ApJS, 112, 315

Magorrian, J., et al. 1998, AJ, 115, 2285

Mahadevan, R. 1997, ApJ, 477, 585

Maoz, E. 1998, ApJ, 494, L181

Narayan, R., Mahadevan, R., & Quataert, E. 1998, in *Theory of Black Hole Accretion Disks*, eds. M. A. Abramowicz, G. Björnsson, & J. E. Pringle (Cambridge: Cambridge University Press), 148

NRAO, 2000, VLA Expansion Project: Phase I - The Ultrasensitive Array

Tanaka, Y., Inoue, H., & Holt, S. S. 1994, PASJ, 46, L37

Thompson, A. R., Clark, B. G., Wade, C. M., Napier, P. J., 1980, ApJS, 44, 151

Wrobel, J. M. 1991, AJ, 101, 127

Wrobel, J. M., & Heeschen, D. S. 1991, AJ, 101, 148

Yi, I., & Boughn, S. P. 1998, ApJ, 499, 198

Table 1. Quiescent Elliptical Galaxies at 8.5 GHz

Symbol	Units	NGC 4291	NGC 4564	NGC 4621	NGC 4660	Reference
$\theta_{\rm M}$	$'$	2.0	2.6	4.5	2.4	1
$\sigma_{\rm DSS}$	$''$	1.7	2.0	3.0	1.8	2
$R_{8.5{\rm GHz}}$	$'',''^{\circ}$	15.4,8.4,+56	10.5,9.0,-22	10.2,9.0,+19	14.7,9.1,+54	3
$\sigma_{8.5{\rm GHz}}$	μJy ba^{-1}	16	13	13	14	3
$S_{8.5{\rm GHz}}$	μJy ba^{-1}	< 64	< 52	153 ± 14	143 ± 15	3
D	Mpc	28.6	15.3	15.3	15.3	4
s	pc/$''$	139	74	74	74	4
$P_{8.5{\rm GHz}}$	W Hz^{-1}	$< 6.3\times10^{18}$	$< 1.5\times10^{18}$	$\leq 4.3\times10^{18}$	$\leq 4.0\times10^{18}$	3
m_8	$10^8 M_\odot$	19	2.5	2.8	2.8	4
$\dot{m}_{\rm A}$		$< 1.6\times10^{-4}$	$< 3.6\times10^{-4}$	$\leq 7.8\times10^{-4}$	$\leq 7.4\times10^{-4}$	3
$\dot{M}_{\rm E}$	$M_\odot$ yr^{-1}	42.	5.5	6.2	6.2	4
$\dot{M}_{\rm A}$	$M_\odot$ yr^{-1}	< 0.007	< 0.002	≤ 0.005	≤ 0.005	3
$L_{\rm RASS}$	erg s^{-1}	8.0×10^{40}	$< 4.2\times10^{39}$	$< 4.6\times10^{39}$	$< 3.9\times10^{39}$	5
$L_{\rm A,1keV}$	erg s^{-1}	$< 5.9\times10^{38}$	$< 4.0\times10^{38}$	$\leq 2.1\times10^{39}$	$\leq 1.9\times10^{39}$	3
$L_{\rm A,6keV}$	erg s^{-1}	$< 3.5\times10^{39}$	$< 2.3\times10^{39}$	$\leq 1.2\times10^{40}$	$\leq 1.1\times10^{40}$	3
$r_{\rm B}$	pc	82	11	12	12	4,6
$\dot{M}_{\rm B}$	$M_\odot$ yr^{-1}	$0.07-0.7$	$0.001-0.01$	$0.001-0.01$	$0.001-0.01$	4,6

References. — (1) Wrobel 1991; (2) Cotton et al. 1999; (3) This work; (4) Magorrian et al. 1998; (5) Beuing et al. 1999; (6) Di Matteo et al. 2000.

Fig. 1.— VLA images of Stokes I emission from the inner $\pm 1'$ of four elliptical galaxies at a frequency of 8.5 GHz. Contour levels are at multiples of the bottom contour level, which is twice the image rms value, $\sigma_{8.5\mathrm{GHz}}$. Hatched ellipses show the restoring beam areas at FWHM. Negative contours are dashed and positive ones are solid. *Upper left:* NGC 4291. *Upper right:* NGC 4564. *Lower left:* NGC 4621. *Lower right:* NGC 4660.

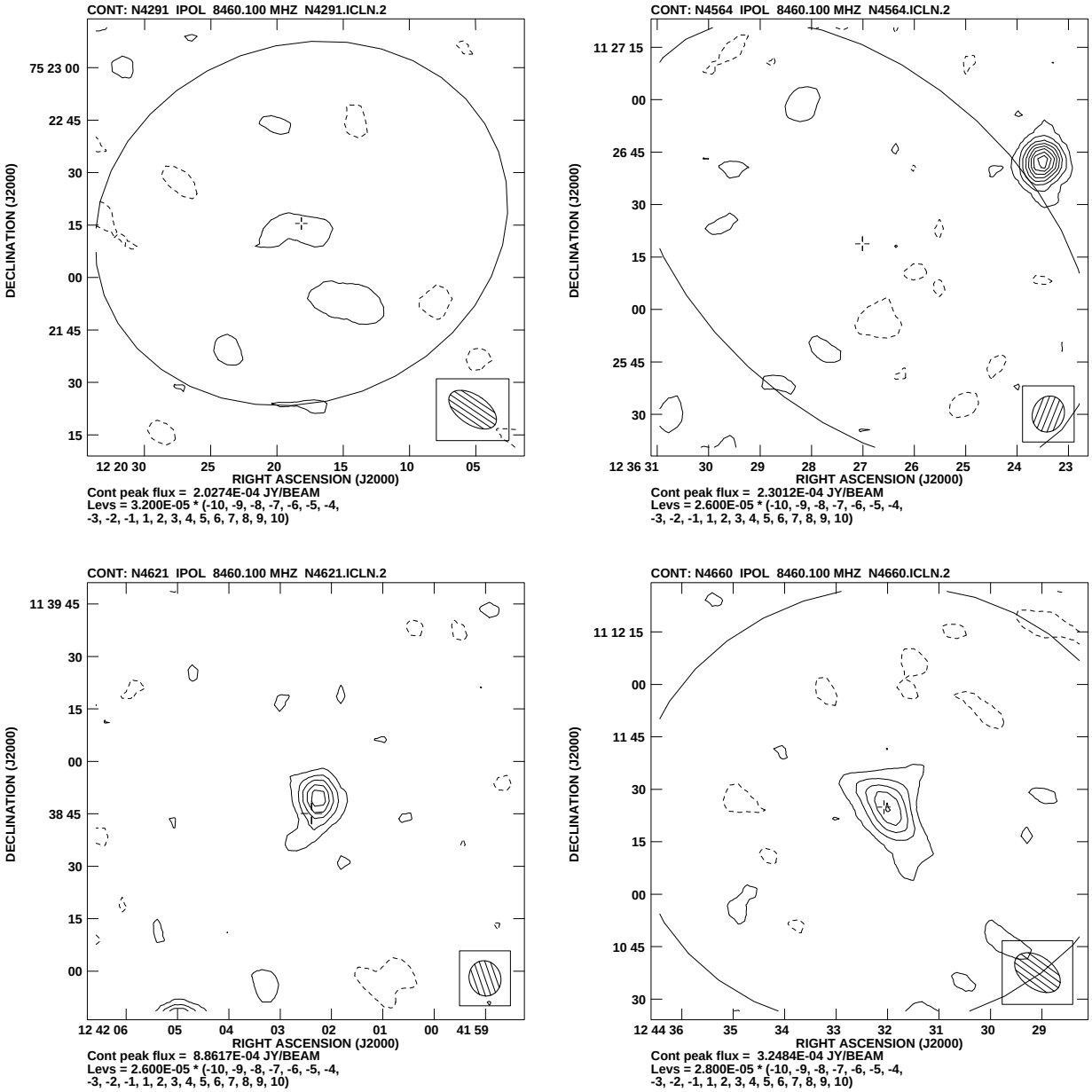
CONT: N4291 IPOL 8460.100 MHZ N4291.ICLN.2
DECLINATION (J2000)
75 23 00
22 45
30
15
00
21 45
30
15
12 20 30
25
20
15
10
05
RIGHT ASCENSION (J2000)
Cont peak flux = 2.0274E-04 JY/BEAM
Levs = 3.200E-05 * (-10, -9, -8, -7, -6, -5, -4,
-3, -2, -1, 1, 2, 3, 4, 5, 6, 7, 8, 9, 10)
CONT: N4564 IPOL 8460.100 MHZ N4564.ICLN.2
DECLINATION (J2000)
11 27 15
00
26 45
30
15
00
25 45
30
12 36 31
30
29
28
27
26
25
24
23
RIGHT ASCENSION (J2000)
Cont peak flux = 2.3012E-04 JY/BEAM
Levs = 2.600E-05 * (-10, -9, -8, -7, -6, -5, -4,
-3, -2, -1, 1, 2, 3, 4, 5, 6, 7, 8, 9, 10)
CONT: N4621 IPOL 8460.100 MHZ N4621.ICLN.2
DECLINATION (J2000)
11 39 45
30
15
00
38 45
30
15
00
12 42 06
05
04
03
02
01
00
41 59
RIGHT ASCENSION (J2000)
Cont peak flux = 8.8617E-04 JY/BEAM
Levs = 2.600E-05 * (-10, -9, -8, -7, -6, -5, -4,
-3, -2, -1, 1, 2, 3, 4, 5, 6, 7, 8, 9, 10)
CONT: N4660 IPOL 8460.100 MHZ N4660.ICLN.2
DECLINATION (J2000)
11 12 15
00
11 45
30
15
00
10 45
30
12 44 36
35
34
33
32
31
30
29
RIGHT ASCENSION (J2000)
Cont peak flux = 3.2484E-04 JY/BEAM
Levs = 2.800E-05 * (-10, -9, -8, -7, -6, -5, -4,
-3, -2, -1, 1, 2, 3, 4, 5, 6, 7, 8, 9, 10)

Figure 1